

QCD Predictions for Charm and Bottom Production at RHIC

R. Vogt

Nuclear Science Division, Lawrence Berkeley National Laboratory, Berkeley, CA 94720, USA

Physics Department, University of California, Davis, CA 95616, USA

In collaboration with M. Cacciari and P. Nason, hep-ph/0502203

Charm as a Probe of Heavy Ion Collisions

Hard probe produced in the initial nucleon-nucleon collisions

Interacts strongly so its momentum can be modified by collisions during the evolution of the system leading to effects such as

- Energy loss in dense matter (Djordjevic et al, Lin et al, Kharzeev and Dokshitzer)
- Transverse momentum broadening due to hadronization from quark-gluon plasma (Svetitsky) or cold nuclear matter
- Collective flow of charm quarks (Lin and Molnar, Rapp et al)

In addition, if multiple $c\bar{c}$ pairs are produced in a given event, can enhance J/ψ (hidden charm) production (Thews et al)

pp and d+Au collisions serve as an important baseline for understanding medium effects on charm production, need good theoretical background and up-to-date open charm data

Charm Hadrons

Open charm hadron production and decay can be detected both through lepton channels (semi-leptonic decays) and through pure hadronic channels (reconstruction of the D mass, momentum)

Measuring D mesons alone is not enough to get total $c\bar{c}$ cross section

| C | Mass (GeV) | $c\tau$ (μm) | $B(C \rightarrow lX)$ (%) | $B(C \rightarrow \text{Hadrons})$ (%) |
|----------------------------|------------|---------------------------|---------------------------|---|
| $D^+(c\bar{d})$ | 1.869 | 315 | 17.2 | $K^-\pi^+\pi^+$ (9.1) |
| $D^-(\bar{c}d)$ | 1.869 | 315 | 17.2 | $K^+\pi^-\pi^-$ (9.1) |
| $D^0(c\bar{u})$ | 1.864 | 123.4 | 6.87 | $K^-\pi^+$ (3.8) |
| $\overline{D^0}(\bar{c}u)$ | 1.864 | 123.4 | 6.87 | $K^+\pi^-$ (3.8) |
| $D^{*\pm}$ | 2.010 | | | $D^0\pi^\pm$ (67.7), $D^\pm\pi^0$ (30.7) |
| D^{*0} | 2.007 | | | $D^0\pi^0$ (61.9) |
| $D_s^+(c\bar{s})$ | 1.969 | 147 | 8 | $K^+K^-\pi^+$ (4.4), $\pi^+\pi^+\pi^-$ (1.01) |
| $D_s^-(\bar{c}s)$ | 1.969 | 147 | 8 | $K^+K^-\pi^-$ (4.4), $\pi^+\pi^-\pi^-$ (1.01) |
| $\Lambda_c^+(udc)$ | 2.285 | 59.9 | 4.5 | ΛX (35), $pK^-\pi^+$ (2.8) |
| $\Sigma_c^{++}(uuc)$ | 2.452 | | | $\Lambda_c^+\pi^+$ (100) |
| $\Sigma_c^+(udc)$ | 2.451 | | | $\Lambda_c^+\pi^0$ (100) |
| $\Sigma_c^0(ddc)$ | 2.452 | | | $\Lambda_c^+\pi^-$ (100) |
| $\Xi_c^+(usc)$ | 2.466 | 132 | | $\Sigma^+K^-\pi^+$ (1.18) |
| $\Xi_c^0(dsc)$ | 2.472 | 29 | | $\Xi^-\pi^+$ (seen) |

Table 1: Ground state charm hadrons with their mass, decay length (when given) and branching ratios to leptons (when applicable) and some prominent decays to hadrons, preferably to only charged hadrons although such decays are not always available.

Bottom Hadrons

Open bottom production and decay can also be detected both through lepton channels (semi-leptonic decays) and through pure hadronic channels (reconstruction of the B mass, momentum)

J/ψ decay channel is often used to obtain B cross section since J/ψ is “easy” to detect

Hadronic branching ratios small, two body decays to charged hadrons rare, harder to measure

B decays contribute to lepton spectra in two ways: direct ($B \rightarrow lX$) and indirect ($B \rightarrow DX \rightarrow lX'$)

Not much information on bottom baryons

| C | Mass (GeV) | $c\tau$ (μm) | $B(C \rightarrow lX)$ (%) | $B(C \rightarrow \text{Hadrons})$ (%) |
|-----------------------|------------|---------------------------|---------------------------|---|
| $B^+(u\bar{b})$ | 5.2790 | 501 | 10.2 | $\bar{D}^0 \pi^- \pi^+ \pi^+$ (1.1), $J/\psi K^+$ (0.1) |
| $B^-(\bar{u}b)$ | 5.2790 | 501 | 10.2 | $D^0 \pi^+ \pi^- \pi^-$ (1.1), $J/\psi K^-$ (0.1) |
| $B^0(d\bar{b})$ | 5.2794 | 460 | 10.5 | $D^- \pi^+$ (0.276), $J/\psi K^+ \pi^-$ (0.0325) |
| $\bar{B}^0(\bar{d}b)$ | 5.2794 | 460 | 10.5 | $D^+ \pi^-$ (0.276), $J/\psi K^- \pi^+$ (0.0325) |
| B_s^0 | 5.3696 | 438 | | $D_s^- \pi^+$ (< 13) |
| $B_c^+(c\bar{b})$ | 6.4 | | | $J/\psi \pi^+$ (0.0082) |
| $B_c^-(\bar{c}b)$ | 6.4 | | | $J/\psi \pi^-$ (0.0082) |
| $\Lambda_b^0(udb)$ | 5.624 | 368 | | $J/\psi \Lambda$ (0.047), $\Lambda_c^+ \pi^-$ (seen) |

Table 2: Known ground state bottom hadrons with their mass, decay length (when given), branching ratios to leptons (when applicable) and some selected decays to hadrons.

Calculating Heavy Flavors in Perturbative QCD

‘Hard’ processes have a large scale in the calculation that makes perturbative QCD applicable: high momentum transfer, μ^2 , high mass, m , high transverse momentum, p_T , since $m \neq 0$, heavy quark production is a ‘hard’ process

Asymptotic freedom assumed to calculate the interactions between two hadrons on the quark/gluon level but the confinement scale determines the probability of finding the interacting parton in the initial hadron

Factorization assumed between the perturbative hard part and the universal, nonperturbative parton distribution functions

The hadronic cross section in an AB collision where $AB = pp, pA$ or nucleus-nucleus is

$$\begin{aligned} \sigma_{AB}(S, m^2) = & \sum_{i,j=q,\bar{q},g} \int_{4m_Q^2/s}^1 \frac{d\tau}{\tau} \int dx_1 dx_2 \delta(x_1 x_2 - \tau) \\ & \times f_i^A(x_1, \mu_F^2) f_j^B(x_2, \mu_F^2) \hat{\sigma}_{ij}(s, m^2, \mu_F^2, \mu_R^2) \end{aligned}$$

f_i^A are the nonperturbative parton distributions, determined from fits to data, x_1 and x_2 are the fractional momentum of hadrons A and B carried by partons i and j , $\tau = s/S$

$\hat{\sigma}_{ij}(s, m^2, \mu_F^2, \mu_R^2)$ is hard partonic cross section calculable in QCD in powers of α_s^{2+n} : leading order (LO), $n = 0$; next-to-leading order (NLO), $n = 1 \dots$

Results depend strongly on quark mass, m , factorization scale, μ_F , in the parton densities and renormalization scale, μ_R , in α_s

Choosing Parameters

Two important parameters: the quark mass m and the scale μ – at high energies, far from threshold, the low x , low μ behavior of the parton densities determines the charm result, bottom less sensitive to parameter choice

The scale is usually chosen so that $\mu_F = \mu_R$, as in parton density fits, no strict reason for doing so for heavy flavors

Two ways to make predictions:

Fit to Data (RV, Hard Probes Collaboration): fix m and $\mu \equiv \mu_F = \mu_R \geq m$ to data at lower energies and extrapolate to unknown regions – tends to favor lower charm masses

Uncertainty Band (Cacciari, Nason and RV): band determined from mass range, $1.3 < m < 1.7$ GeV (charm) and $4.5 < m < 5$ GeV (bottom) with $\mu_F = \mu_R = m$, and range of scales relative to central mass value, $m = 1.5$ GeV (charm) and 4.75 GeV (bottom): $(\mu_F/m, \mu_R/m) = (1, 1), (2, 2), (0.5, 0.5), (0.5, 1), (1, 0.5), (1, 2), (2, 1)$ (Ratio is relative to m_T for distributions)

Need to be careful with $\mu_F \leq m$ and the CTEQ6M parton densities since $\mu_{\min} 1.3$ GeV, gives big K factors for low scales – problem occurs at low p_T

Densities like GRV98 have lower μ_{\min} so low x , low μ behavior less problematic

Value of two-loop α_s is big for low scales, for $m = 1.5$ GeV:

$$\alpha_s(m/2 = 0.75 \text{ GeV}) = 0.648, \alpha_s(m = 1.5 \text{ GeV}) = 0.348 \text{ and } \alpha_s(2m = 3 \text{ GeV}) = 0.246$$

CTEQ6M Densities at $\mu = m/2, m$ and $2m$

CTEQ6M densities extrapolate to $\mu < \mu_{\min} = 1.3$ GeV

When backwards extrapolation leads to $xg(x, \mu) < 0$, then $xg(x, \mu) \equiv 0$

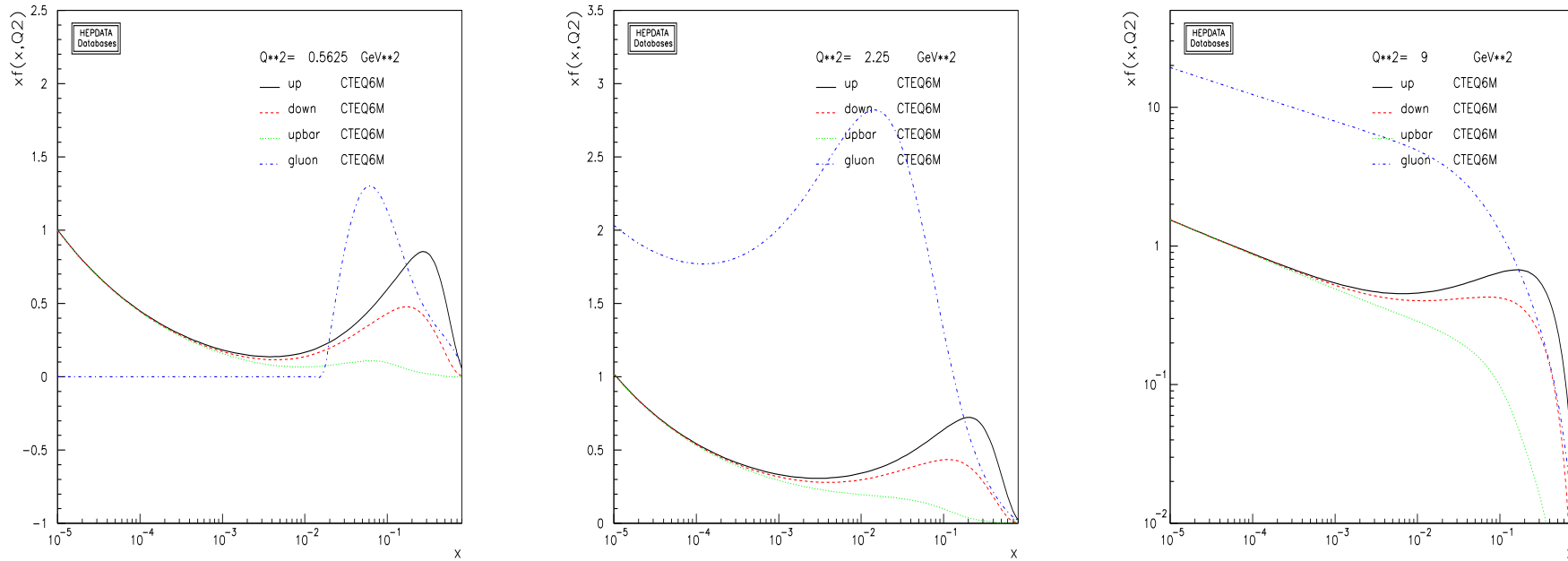


Figure 1: The CTEQ6M parton densities as a function of x for $\mu = m/2$ (left), $\mu = m$ (middle) and $\mu = 2m$ (right) for $m = 1.5$ GeV.

FONLL Calculation (Cacciari and Nason)

Designed to cure large logs of p_T/m for $p_T \gg m$ in fixed order calculation (FO) where mass is no longer only relevant scale

Includes resummed terms (RS) of order $\alpha_s^2(\alpha_s \log(p_T/m))^k$ (leading log – LL) and $\alpha_s^3(\alpha_s \log(p_T/m))^k$ (NLL) while subtracting off fixed order terms retaining only the logarithmic mass dependence (the “massless” limit of fixed order (FOM0)), both calculated in the same renormalization scheme

Scheme change needed in the FO calculation since it treats the heavy flavor as heavy while the RS approach includes the heavy flavor as an active light degree of freedom

Schematically:

$$\text{FONLL} = \text{FO} + (\text{RS} - \text{FOM0}) G(m, p_T)$$

$G(m, p_T)$ is arbitrary but $G(m, p_T) \rightarrow 1$ as $m/p_T \rightarrow 0$ up to terms suppressed by powers of m/p_T

Total cross section similar to but slightly higher than NLO

Problems at high energies away from midrapidity due to small x , high z behavior of fragmentation functions in RS result, therefore we don't calculate results for $|y| > 2$, worse for LHC predictions

Comparison of FONLL and NLO p_T Distributions

FONLL result for bare charm is slightly higher over most of the p_T range – fixed order result gets higher at large p_T due to large $\log(p_T/m)$ terms

New D^0 fragmentation functions (dashed) harder than Peterson function (dot-dot-dot-dashed)

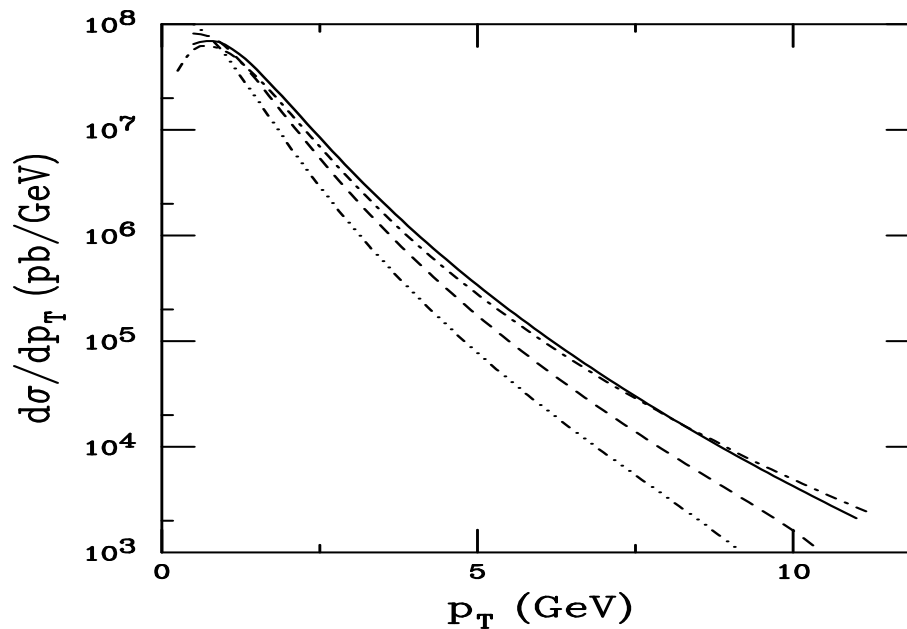


Figure 2: The p_T distributions calculated using FONLL are compared to NLO. The dot-dashed curve is the NLO charm quark p_T distribution. The solid, dashed and dot-dot-dot-dashed curves are FONLL results for the charm quark and D^0 meson with the updated fragmentation function and the Peterson function, respectively. All the calculations are done with the CTEQ6M parton densities, $m = 1.2$ GeV and $\mu = 2m_T$ in the region $|y| \leq 0.75$.

Uncertainty Bands for p_T Distributions

Due to range of parameters chosen for uncertainty band, the maximum and minimum result as a function of p_T may not come from a single set of parameters

Thus the upper and lower curves in the band do not represent a single set of μ_R , μ_F and m values but are the upper and lower limits of mass and scale uncertainties added in quadrature:

$$\frac{d\sigma_{\max}}{dp_T} = \frac{d\sigma_{\text{cent}}}{dp_T} + \sqrt{\left(\frac{d\sigma_{\mu,\max}}{dp_T} - \frac{d\sigma_{\text{cent}}}{dp_T}\right)^2 + \left(\frac{d\sigma_{m,\max}}{dp_T} - \frac{d\sigma_{\text{cent}}}{dp_T}\right)^2}$$

$$\frac{d\sigma_{\min}}{dp_T} = \frac{d\sigma_{\text{cent}}}{dp_T} - \sqrt{\left(\frac{d\sigma_{\mu,\min}}{dp_T} - \frac{d\sigma_{\text{cent}}}{dp_T}\right)^2 + \left(\frac{d\sigma_{m,\min}}{dp_T} - \frac{d\sigma_{\text{cent}}}{dp_T}\right)^2}$$

The central values are $m = 1.5$ GeV (charm) and 4.75 GeV (bottom), $\mu_F = \mu_R = m_T$

We follow the same procedure for both the NLO and FONLL calculations and compare them in the central ($|y| \leq 0.75$) and forward ($1.2 < y < 2.2 - 1.2 < y < 2$ for FONLL) regions

Previous (HPC) charm results with $m = 1.2$ GeV, $\mu_F = \mu_R = 2m_T$ fall within the uncertainty band

Bare heavy quark and heavy flavor meson p_T distributions shown for pp collisions at $\sqrt{S} = 200$ and 500 GeV

Components of Uncertainty Band at NLO

Curves with $(\mu_F/m_T, \mu_R/m_T) = (1, 0.5)$ and $(0.5, 0.5)$ define the maximum of the band with $(0.5, 1)$ and $(2, 2)$ form the minimum

Turnover of minimum at low p_T because $\mu_F < \mu_{\min}$ of CTEQ6M

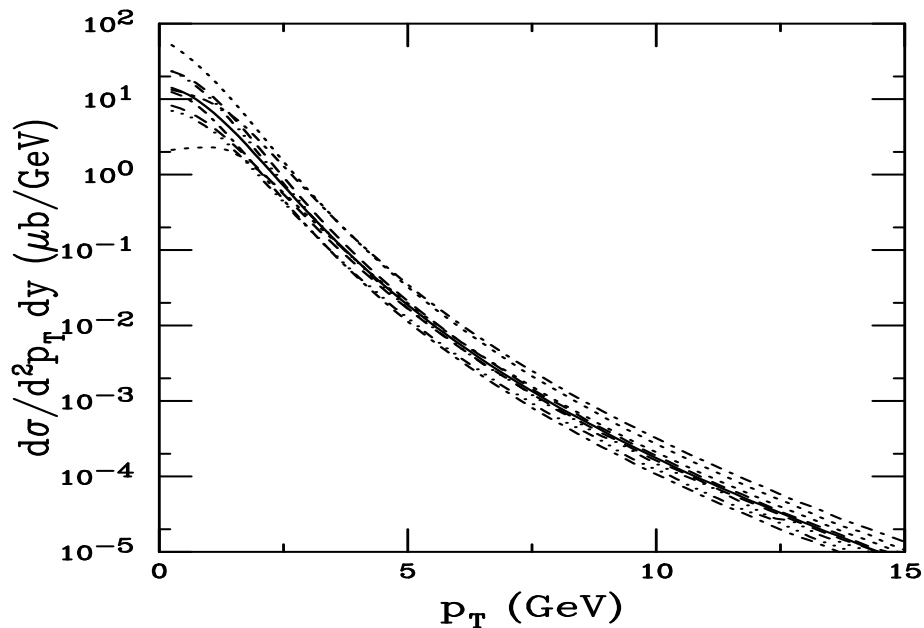


Figure 3: The charm quark p_T distributions calculated using CTEQ6M. The solid curve is the central value $(\mu_F/m_T, \mu_R/m_T) = (1, 1)$ with $m = 1.5$ GeV. The upper and lower dashed curves are $m = 1.3$ and 1.7 GeV with $(1, 1)$ respectively. The upper and lower dot-dashed curves correspond to $(0.5, 0.5)$ and $(2, 2)$ while the upper and lower dotted curves are with $(1, 0.5)$ and $(0.5, 1)$ and the upper and lower dot-dot-dot-dashed curves are with $(2, 1)$ and $(1, 2)$ with $m = 1.5$ GeV.

Uncertainty Bands for c and D at 200 GeV

NLO and FONLL bands very similar to each other

D meson band calculated for primary D s

Not possible to separate c and D bands for $p_T < 10$ GeV – looks more like a delta function

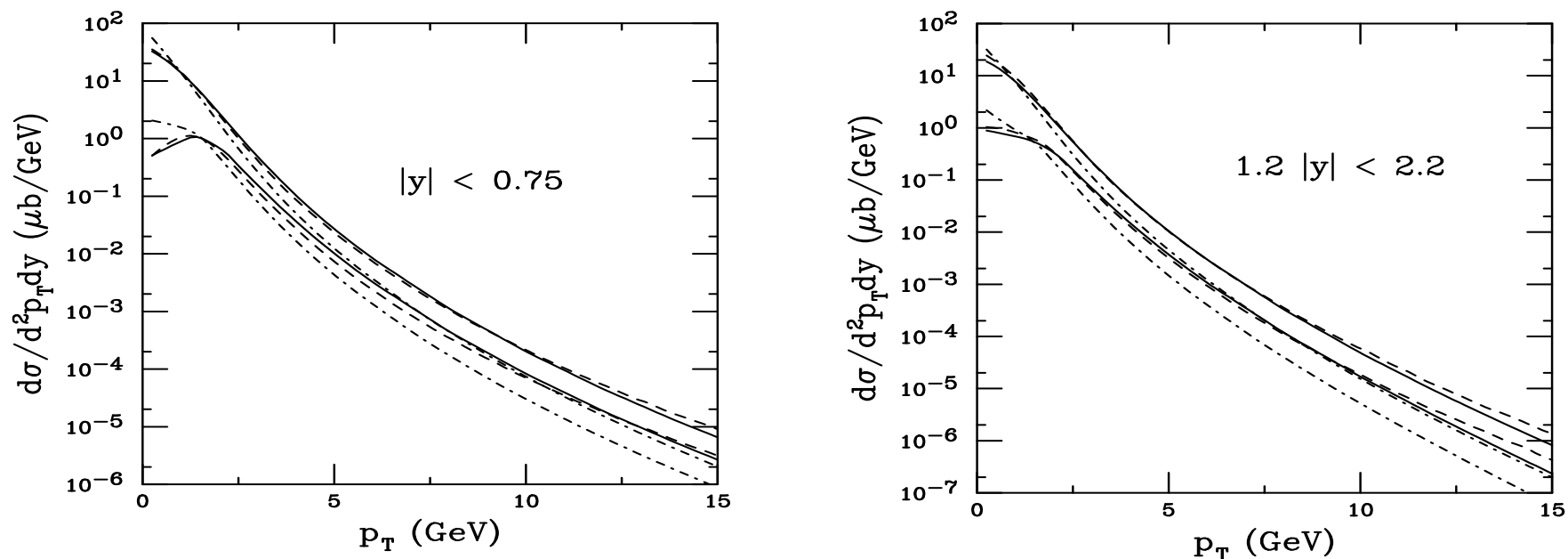


Figure 4: The charm quark theoretical band as a function of p_T for FONLL (solid curves) and NLO (dashed curves) in $\sqrt{S} = 200$ GeV pp collisions. Also shown is the D meson uncertainty band, all using the CTEQ6M parton densities. The left-hand plot gives the result for $|y| \leq 0.75$ while the right-hand plot shows the result for $1.2 \leq |y| \leq 2.2$.

Comparison to STAR d+Au D Data

Agreement of upper limit of uncertainty band with low p_T STAR data rather reasonable

Change in slope relative to data above $p_T \sim 2.5$ GeV

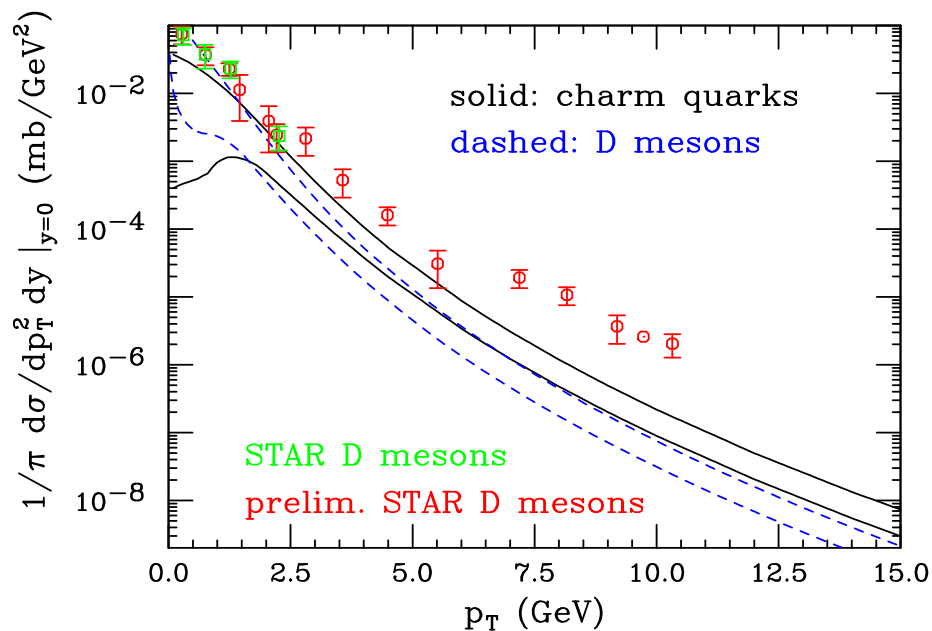


Figure 5: The FONLL theoretical uncertainty bands for the charm quark and D meson p_T distributions in pp collisions at $\sqrt{S} = 200$ GeV, using $\text{BR}(c \rightarrow D) = 1$. Both final and preliminary STAR d+Au data (scaled to pp using $N_{\text{bin}} = 7.5$) at $\sqrt{S_{NN}} = 200$ GeV are also shown.

Uncertainty Bands for c and D at 500 GeV

Uncertainty band broader at low p_T due to smaller x region reached for $\mu_F < \mu_{\min}$ of PDF

c and D distributions are harder at 500 GeV

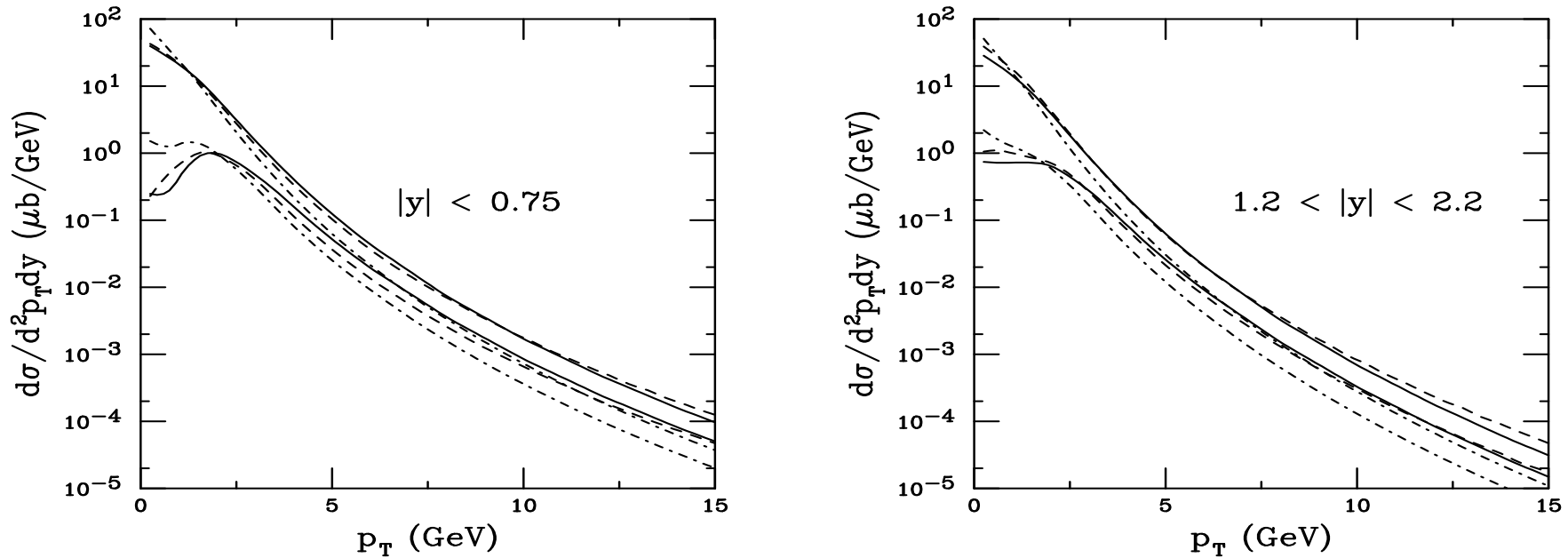


Figure 6: The charm quark theoretical band as a function of p_T for FONLL (solid curves) and NLO (dashed curves) in $\sqrt{S} = 500$ GeV pp collisions. Also shown is the D meson uncertainty band, all using the CTEQ6M parton densities. The left-hand plot gives the result for $|y| \leq 0.75$ while the right-hand plot shows the result for $1.2 \leq |y| \leq 2.2$.

Uncertainty Bands for b and B at 200 GeV

Bands narrower for bottom than for charm

Impossible to separate b from B over the p_T range shown (B is a generic B meson)

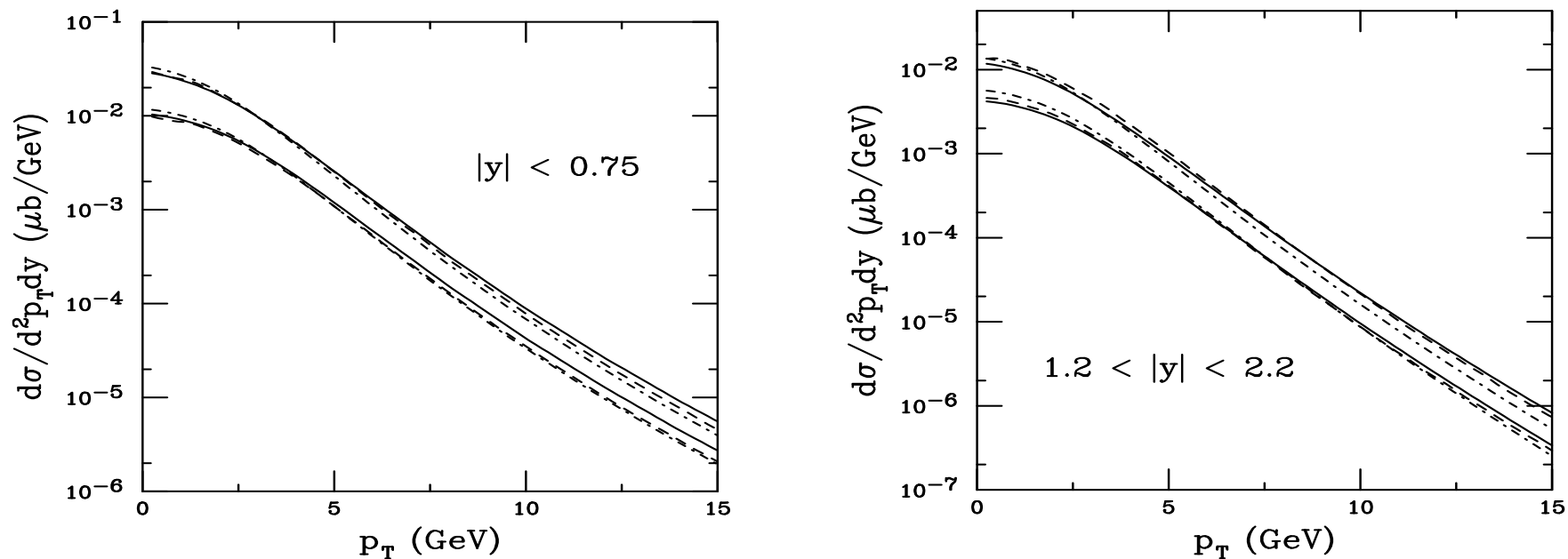


Figure 7: The bottom quark theoretical band as a function of p_T for FONLL (solid curves) and NLO (dashed curves) in $\sqrt{S} = 200$ GeV pp collisions. Also shown is the B meson uncertainty band, all using the CTEQ6M parton densities. The left-hand plot gives the result for $|y| \leq 0.75$ while the right-hand plot shows the result for $1.2 \leq |y| \leq 2.2$.

Uncertainty Bands for b and B at 500 GeV

Much stronger energy dependence and more hardening for bottom than for charm with increasing energy

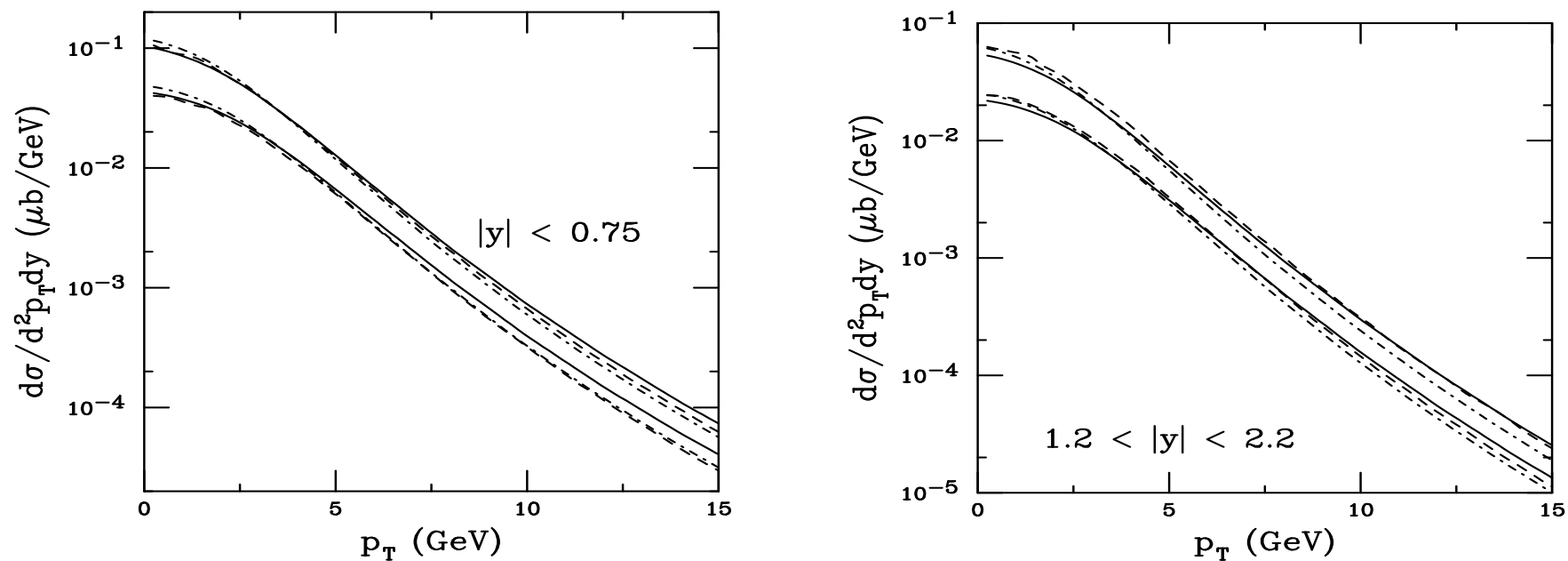


Figure 8: The bottom quark theoretical band as a function of p_T for FONLL (solid curves) and NLO (dashed curves) in $\sqrt{S} = 500$ GeV pp collisions. Also shown is the B meson uncertainty band, all using the CTEQ6M parton densities. The left-hand plot gives the result for $|y| \leq 0.75$ while the right-hand plot shows the result for $1.2 \leq |y| \leq 2.2$.

Obtaining the Electron Spectra From Heavy Flavor Decays

D and B decays to leptons depends on measured decay spectra and branching ratios

$D \rightarrow e$ Use preliminary CLEO data on inclusive electrons from semi-leptonic D decays, assume it to be identical for all charm hadrons

$B \rightarrow e$ Primary B decays to electrons measured by Babar and CLEO, fit data and assume fit to work for all bottom hadrons

$B \rightarrow D \rightarrow e$ Obtain electron spectrum from convolution of $D \rightarrow e$ spectrum with parton model calculation of $b \rightarrow c$ decay

Branching ratios are admixtures of charm and bottom hadrons

$$B(D \rightarrow e) = 10.3 \pm 1.2 \%$$

$$B(B \rightarrow e) = 10.86 \pm 0.35 \%$$

$$B(B \rightarrow D \rightarrow e) = 9.6 \pm 0.6 \%$$

Uncertainty Bands for Electrons from Heavy Flavor Decays at 200 GeV

Electrons from B decays begin to dominate at $p_T \sim 5$ GeV

Electron spectra very sensitive to rapidity range – to get $|y| \leq 0.75$ electrons, need $|y| \leq 2$ charm and bottom range

Forward electron spectra thus not possible to obtain using FONLL code due to problems at large y

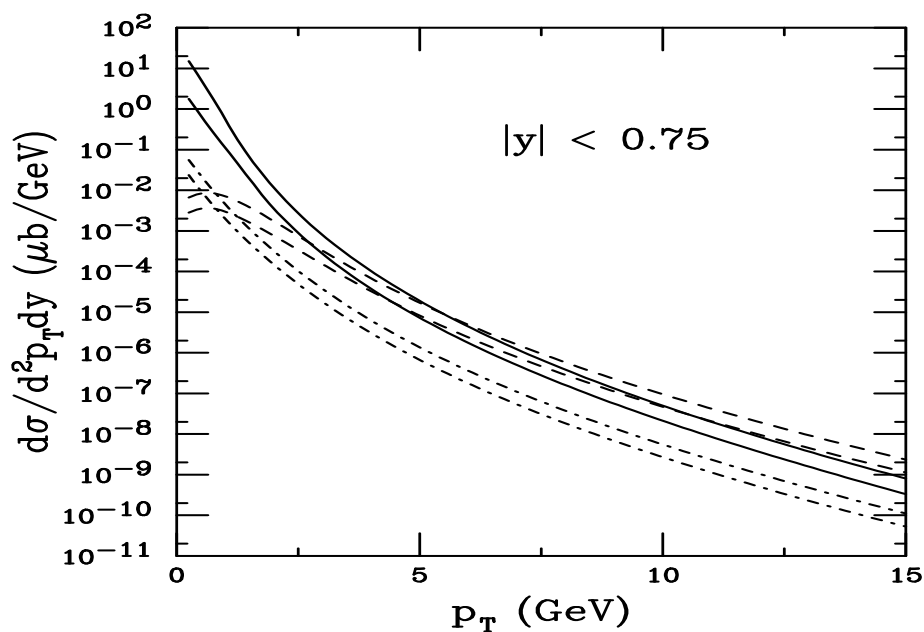


Figure 9: The theoretical FONLL bands for $D \rightarrow eX$ (solid), $B \rightarrow eX$ (dashed) and $B \rightarrow DX \rightarrow eX'$ (dot-dashed) as a function of p_T in $\sqrt{S} = 200$ GeV pp collisions for $|y| < 0.75$.

Comparison to Electron Data at 200 GeV

Includes PHENIX preliminary data from pp and STAR published and preliminary data

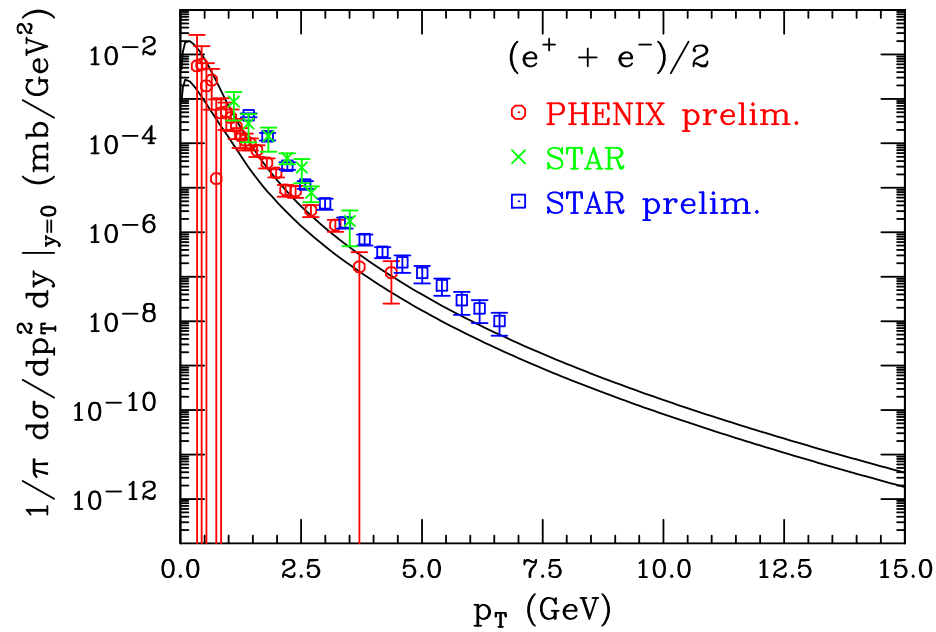


Figure 10: Prediction of the theoretical uncertainty band of the total electron spectrum from charm and bottom (Cacciari, Nason and RV). Preliminary data from PHENIX and STAR are also shown.

Uncertainty Bands for Electrons from Heavy Flavor Decays at 500 GeV

Crossover between D and B dominance is similar at the higher energy

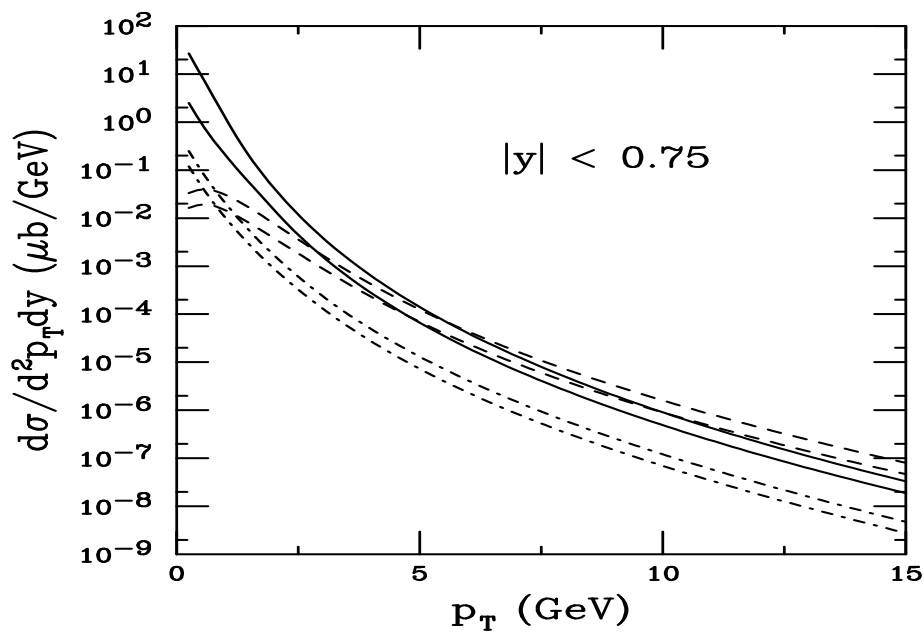


Figure 11: The theoretical FONLL bands for $D \rightarrow eX$ (solid), $B \rightarrow eX$ (dashed) and $B \rightarrow DX \rightarrow eX'$ (dot-dashed) as a function of p_T in $\sqrt{S} = 500$ GeV pp collisions for $|y| < 0.75$.

Summary

- The FONLL calculation of heavy quark production is used to better predict the p_T dependence at collider energy – cures large logs of p_T/m
- Includes more modern fragmentation functions for D and B mesons – meson and quark distributions similar at higher p_T than previously obtained from older e^+e^- fits
- Contributions of D and B decays to leptons difficult to disentangle, requires reconstruction of hadronic decays to distinguish between them